Robust Semi-Blind Packing Ratio Estimation for Faster-Than-Nyquist Signaling

Qiang Li, *Member, IEEE*, Liping Li , *Member, IEEE*, Xingwang Li, *Senior Member, IEEE*, Octavia A. Dobre, *Fellow, IEEE*, Ming Zeng, *Member, IEEE*, Yingsong Li, *Senior Member, IEEE*, and Yan Wang

***Abstract*— Accurate packing ratios are indispensable for the faster-than-Nyquist (FTN) signaling; therefore, we propose two robust semi-blind packing ratio estimation algorithms in this letter. Concretely, we construct a pilot-based FTN transmission scheme over the channel with frequency offset and phase noise. We conduct correlation operations on downsampled pilots, assuming a predetermined downsampling factor. To mitigate the impacts of frequency offset and phase noise, we employ differential post-detection integration (DPDI) and differential-generalized post-detection integration (DGPDI) for correlation operations. The packing ratio is estimated by selecting the downsampling factor corresponding to the maximum decision value. Simulation results demonstrate that the coherent correlation yields optimal estimation accuracy in the absence of frequency offset and phase noise. Otherwise, the estimation algorithms using DPDI and DGPDI, i.e., PRE-DPDI and PRE-DGPDI, realize higher estimation accuracy than that using the coherent correlation. When the packing ratio and the normalized frequency offset are 0.8 and 0.2, signal-to-noise ratios required for PRE-DPDI and PRE-DGPDI to achieve a probability of false alarm of 10^{-4} are about 7 and 3 dB, respectively.**

***Index Terms*— Faster-than-Nyquist, frequency offset, packing ratio estimation, phase noise, post-detection integration.**

I. Introduction

SINCE Mazo demonstrated that packing the symbol period to a specific extent does not necessarily decrease the theoretical bit error ratio [1], faster-than-Nyquist (FTN) signaling, as a physical layer technique, has gained considerable attention for its potential to improve the capacities and the spectrum efficiencies of communication systems [2]. However, deviating from the Nyquist criterion makes the FTN signaling introduce inter-symbol interference (ISI), thus leading to two directions of research on the FTN signaling.

On one hand, the signal detection algorithms are indispensable to ensure the reliability of the FTN signaling. These mainly involve Bahl-Cocke-Jelinek-Raviv (BCJR) [3], iterative interference cancellation [4], equalization [5] and precoding [6]. For example, to recover the transmitted symbols, the precoding algorithms utilized the ISI matrix decomposition to construct their precoding and decoding matrices. These signal detection algorithms for the FTN signaling, except for the time-domain equalization algorithm, assumed precise knowledge of the packing ratio at the receiver by means of the control frame or the preset method.

On the other hand, regarding the FTN-induced ISI as artificial noise, the FTN signaling was used for the physical layer security [7]. Using a predetermined pattern of filter hopping, the pulse shaping filter in the transmitter varied over time within the FTN signaling framework [8]. Further, the FTN signaling scheme using variable packing ratios was considered for the physical layer security [9], which presented the capacities for both the cooperative and non-cooperative links. Besides, the secrecy rate and secrecy outage probability of the FTN signaling over a frequency-flat Rayleigh fading channel were derived [10]. The above studies assumed that the packing ratio patterns had been determined or synchronized between the receiver and transmitter when the FTN systems were established. A blind packing ratio estimation based on deep learning was proposed for the FTN signaling [11], which was thereafter applied in a variable packing ratio transmission system [12]. However, its high complexity and sensitivity to frequency offset and phase noise made it impractical for the FTN signaling. Based on the cyclostationarity of the FTN signaling [13], low-complexity non-data-aided (NDA) and data-aided (DA) packing ratio estimators (NDA-PRE and DA-PRE) were proposed for FTN signaling [14]. Using uniformly spaced samples of the FTN signal taken at an arbitrary FTN rate, they were robust to the timing phase errors; nevertheless, due to the assumption of the fixed phase offset caused by the frequency offset in the symbols used for estimation, they were only suitable for the FTN signaling with a slight frequency offset. Besides, a high estimation accuracy can only be obtained if the symbol length used for estimation is large enough.

As previously indicated, the accurate packing ratio is necessary for the FTN signaling. If the receivers are unaware of the packing ratios used by the transmitters, signal detection and physical layer security can hardly be achieved. Moreover,

This work was supported in part by National Natural Science Foundation of China under Grant 62071002, and in part by "Double First-Class" Discipline Creation Project of Surveying Science and Technology under Grants CHXKYXBS03 and GCCRC202306. The associate editor coordinating the review of this letter and approving it for publication was C. Tsinos. *(Corresponding author: Liping Li.)*

Qiang Li, Liping Li, Yingsong Li, and Yan Wang are with the School of Electronic and Information Engineering, Anhui University, Hefei 230601, China (e-mail: buaji@ahu.edu.cn; liping_li@ahu.edu.cn; liyingsong@ieee.org; 2217791567@qq.com).

Xingwang Li is with the School of Physics and Electronic Information Engineering, Henan Polytechnic University, Jiaozuo 454000, China (e-mail: lixingwangbupt@gmail.com).

Octavia A. Dobre is with the Faculty of Engineering and Applied Science, Memorial University, St. John's, NL A1B 3X5, Canada (e-mail: odobre@mun.ca).

Ming Zeng is with the Department of Electrical Engineering and Computer Engineering, Université Laval, Québec City, QC G1V 0A6, Canada (e-mail: ming.zeng@gel.ulaval.ca).

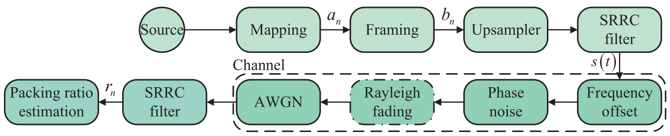

Fig. 1. Pilot-based FTN transceiver.

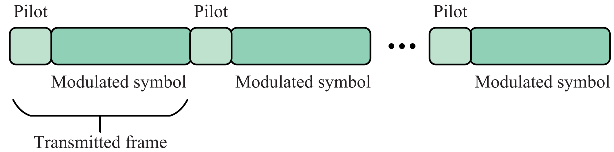

Fig. 2. Framing for the FTN signaling.

when the FTN signaling is used to adapt the transmission rate according to the user's quality-of-service, the packing ratios are random and vary with the real-time demand, which implies that the packing ratio patterns cannot be predetermined or pre-synchronized between the receiver and the transmitter. Besides, for the physical layer security, the FTN signaling using the dynamic packing ratio patterns is more promising than that using the fixed packing ratio patterns. In light of the above considerations, a packing ratio estimation algorithm is indispensable to realize the full potential of the FTN signaling. In addition, since most frequency offset and phase noise elimination algorithms are semi-blind and use pilots after downsampling, they require precise packing ratios. Therefore, packing ratio estimation should precede frequency offset and phase noise elimination and be resilient to these distortions. The existing algorithms fall short of meeting this demand.

In this letter, we propose two robust and high-accuracy packing ratio estimation algorithms for the FTN signaling. They efficiently mitigate the impacts of frequency offset and phase noise. Specifically, we construct a pilot-based FTN transmission scheme over the channel with frequency offset and phase noise. Given the unknown packing ratio, we use all possible downsampling factors and conduct correlation operations on the downsampled pilots. To combat frequency offset and phase noise, we introduce post-detection integration (PDI) into the packing ratio estimation process. The downsampling factor yielding the maximum decision value is determined by comparing all decision values, thereby facilitating the estimation of the packing ratio.

II. Pilot-Based FTN Signaling Over The Channel With Frequency Offset and Phase Noise

A pilot-based FTN transceiver is adopted in this letter, as shown in Fig. 1, where a_n is the modulated symbol with the average power of E_s. Baseband shaping for the FTN signaling involves an upsampler and a T-orthogonal square root raised cosine (SRRC) filter $c(t)$. The upsampling factors of the upsampler and the SRRC filter are denoted by M and U, respectively. In this case, the packing ratio for the FTN signaling is $\alpha = M/U, M \leq U$. The symbol rate can be increased by decreasing the upsampling factor M while keeping the sampling rate after the SRRC filter constant; therefore, different packing ratios, i.e., different upsampling factors, lead to different symbol rates.

The framing process is shown in Fig. 2, where the lengths of the pilot block and the modulated symbol block are L and D, known to the receiver. Generally, the pilot block is composed of fixed symbols, defined as $\mathbf{p} = [p_0, p_1, p_2, \cdots, p_{L-1}]$. The pilots reduce the spectrum efficiency of the FTN signaling; however, this loss could be ignored when the length of the modulated symbol block is relatively large.

Consequently, the k-th transmitted frame is

$$\begin{aligned}\mathbf{b}_k &= [b_{(k-1)(L+D)}, b_{(k-1)(L+D)+1}, \cdots, b_{k(L+D)-1}] \\ &= \left[\mathbf{p}, a_{(k-1)D}, a_{(k-1)D+1}, a_{(k-1)D+2}, \cdots, a_{kD-1}\right]. \end{aligned} \quad (1)$$

Then, the transmitted signal for the FTN signaling is

$$s(t) = \sqrt{\alpha E_s} \sum\nolimits_{n=0}^{N-1} b_n c(t - n\alpha T), \quad (2)$$

where N represents the length of symbols after framing.

Affected by frequency offset, phase noise and additive white Gaussian noise (AWGN), the received signal without Rayleigh fading for the FTN signaling is

$$r(t) = s(t) \exp\left(j\left(2\pi \Delta f t + \varphi(t)\right)\right) + w(t), \quad (3)$$

where Δf indicates the frequency offset, and $\sigma = \Delta f T$ is the normalized frequency offset; $\varphi(t)$ and $w(t)$ represent the phase noise and the AWGN, respectively.

As a consequence, the received symbols through the SRRC filter can be expressed as

$$r_k = \sqrt{\alpha E_s} \sum_{n=0}^{N-1} b_n g\left((k - nM) T_s\right) e^{j(2\pi k \Delta f T_s + \varphi(k T_s))} + w_k, \quad (4)$$

where $T_s = T/U$ represents the sampling rate, and w_k is the colored noise. $g(t) = c(t) \otimes c(t)$ indicates a raised cosine filter, and $\otimes$ represents the linear convolution.

III. Robust Packing Ratio Estimation for FTN Signaling

A. Packing Ratio Estimation

Since the packing ratio is unknown to the receiver, the receiver cannot perform the correct downsampling process. The objective of packing ratio estimation is to obtain the correct downsampling factor from (4).

Like [15], we assume that the receiver performs the perfect synchronization. This assumption is reasonable since the FTN-induced ISI and variations of the packing ratios have little effect on the performance of the semi-blind synchronization algorithms, which generally adopt binary phase shift keying (BPSK)-based pilots and are commonly used in modern communication systems. Considering the packing ratio cannot be obtained before synchronization, correlation-based synchronization is performed on downsampled pilots using all possible downsampling factors. Then, the maximum correlation value for each symbol is used to determine if this symbol is the start of the frame. It is worth mentioning that if one symbol is identified as the start of the frame, the downsampling factor corresponding to the maximum correlation value of this symbol can be used to estimate the packing ratio. Similarly, the semi-blind compensation algorithms for channel or hardware imperfections are almost independent of the FTN-induced ISI and variations of the packing ratios.

If the receiver assumes that the downsampling factor is M', the corresponding packing ratio is calculated as M'/U. In this case, the downsampled symbols are

$$y_k = \sqrt{\alpha E_s} \sum_{n=0}^{N-1} b_n g\left(\left(kM' - nM\right) T_s\right) \exp\left(j\gamma\left(k\right)\right) + w'_k, \tag{5}$$

where the frequency offset and the phase noise are represented as

$$\gamma\left(k\right) = 2\pi k \Delta f M' T_s + \varphi\left(kM'T_s\right). \tag{6}$$

The k-th downsampled pilot block in (5) is defined as

$$\bar{\mathbf{p}}_k = [\bar{p}_{k,0}, \bar{p}_{k,1}, \bar{p}_{k,2}, \cdots, \bar{p}_{k,L-1}], \tag{7}$$

which corresponds to the transmitted pilot block $\mathbf{p}$.

It can be concluded from (5) that the downsampled pilots using the correct packing ratio are quite different from those using the wrong packing ratio. Therefore, if the pilot block is a sequence with high autocorrelation such as the gold sequence, we can use the correlation operation to determine whether the downsampled pilots are the desired symbols. Note that the circular FTN signaling and the cyclic prefix/suffix scheme cannot be achieved due to the uncertainty of the packing ratio. Besides, the accurate FTN-induced ISI matrix is unavailable because the pilots suffer from the ISI caused by the modulated symbols. Therefore, we directly adopt the transmitted pilots, i.e., $\mathbf{p}$, to perform the correlation operation with the downsampled pilots.

Assuming a downsampling factor of M', an intuitive method to perform the decision for the $k-$th downsampled pilot block is the coherent correlation (CC), written as

$$\Lambda_1 = \left|\sum\nolimits_{i=0}^{L-1} \bar{p}_{k,i} p_i\right|. \tag{8}$$

Using (5), (8) is further expressed as

$$\begin{aligned}\Lambda_1 &= \left|\sum\nolimits_{i=0}^{L-1} y_\nu p_i\right| \\ &= \left|\sum\nolimits_{i=0}^{L-1} \left(\tilde{p}_{k,i} p_i \exp\left(j\gamma\left(\nu\right)\right) + w'_\nu p_i\right)\right|,\end{aligned} \tag{9}$$

where $\nu = \left(k-1\right)\left(L+D\right) + i$; $\tilde{p}_{k,i}$ is the downsampled pilot with the FTN-induced ISI only. Equation (9) shows that the packing ratio estimation using CC, referred to as PRE-CC, is unable to mitigate the impacts of frequency offset and phase noise.

Assuming that the phase noise remains unchanged over each pilot block, non-coherent correlation overcomes phase rotation and phase noise, which is

$$\begin{aligned}\bar{p}_{k,i}\bar{p}^*_{k,i+l} &= \left(\tilde{p}_{k,i} e^{j\gamma(\nu)} + w'_\nu\right)\left(\tilde{p}_{k,i+l} e^{j\gamma(\nu+l)} + w'_{\nu+l}\right)^* \\ &= \tilde{p}_{k,i}\tilde{p}^*_{k,i+l} \exp\left(-j2\pi l \Delta f M' T_s\right) + \hat{w},\end{aligned} \tag{10}$$

where $\hat{w}$ represents the noise-induced component, and l is the span of the non-coherent correlation; the superscript $(\cdot)^*$ represents the conjugate operation.

Ignoring the noise-induced component, the differential PDI (DPDI) uses the non-coherent correlation to accumulate the decision value as

$$\begin{aligned}\Lambda_2 &= \left|\sum\nolimits_{i=0}^{L-l-1} \bar{p}_{k,i}\bar{p}^*_{k,i+l}\left(p_i p^*_{i+l}\right)^*\right| \\ &= \left|\sum\nolimits_{i=0}^{L-l-1} \tilde{p}_{k,i}\tilde{p}^*_{k,i+l} e^{-j2\pi l \Delta f M' T_s}\left(p_i p^*_{i+l}\right)^*\right| \\ &= \left|\sum\nolimits_{i=0}^{L-l-1} \tilde{p}_{k,i} p^*_i \tilde{p}^*_{k,i+l} p_{i+l}\right|.\end{aligned} \tag{11}$$

From (10) and (11), it can be observed that the performance of DPDI deteriorates in the presence of noise. Therefore, the performance of the packing ratio estimation using the DPDI is inferior to that of PRE-CC in the absence of frequency offset and phase noise.

To further improve the robustness, the differential-generalized PDI (DGPDI) can be applied as

$$\Lambda_3 = \sum\nolimits_{l=1}^{L-1} \Lambda_2. \tag{12}$$

The packing ratio estimation algorithms using (11) and (12) are referred to as PRE-DPDI and PRE-DGPDI, respectively. The overall flow of the proposed packing ratio estimation algorithms is shown in **Algorithm 1**. Due to the uncertainty of the packing ratio, we use all possible upsampling factors, i.e., $[1, 2, \cdots, U]$, for downsampling and perform the correlation U times, where the upsampling factor corresponding to the largest correlation value is used to estimate the packing ratio.

Algorithm 1 Packing Ratio Estimation Algorithms

Input: the received symbol r_k, the downsampling factor U of the SRRC filter, the transmitted pilots $\mathbf{p}$ and the span l.
Output: the packing ratio $\tilde{\alpha}$.

```
initialization: M' = 1;
while M' ≤ U do
    downsample the received symbols using (5);
    perform the correlation using (8), (11) or (12);
    save the decision value corresponding to M';
    M' = M' + 1;
end
obtain the downsampling factor M̃ corresponding to
  the maximum decision value;
calculate the packing ratio by α̃ = M̃ / U.
```

B. Complexity Analysis

The complexity of the proposed packing ratio estimation algorithms mainly lies in the correlation operations. Each operation of (8) requires L multiplications and one modulo operation. Besides, one multiplication is required to calculate the packing ratio; therefore, the total complexity of the

PRE-CC algorithm is $UL + 1$ multiplications and U modulo operations. Since the PRE-DPDI algorithm requires $3(L - l)$ multiplications and one modulo operation to perform (11), its complexity is $3U(L - l) + 1$ multiplications and U modulo operations. Similarly, the PRE-DGPDI algorithm requires a complexity of $3UL(L-1)/2 + 1$ multiplications and UL modulo operations. By contrast, the PRE-CC algorithm has the lowest complexity while the PRE-DGPDI algorithm has the highest complexity. In addition, the multiplication of the PRE-DPDI and PRE-DGPDI algorithms can be simplified since $p_i p_{i+l}^*$ in (11) can be pre-calculated and stored in memory. In this way, the PRE-DPDI and PRE-DGPDI algorithms require $2U(L - l) + 1$ and $UL(L - 1) + 1$ multiplications, respectively. Moreover, DA-PRE's complexity mainly depends on its calculation of second-order moment [14], which requires K multiplications, with K indicating the length of symbols used for DA-PRE. When K equals L, DA-PRE has lower complexity than the proposed packing ratio estimation algorithms. It should be mentioned that DA-PRE requires a much larger K than L to obtain a high estimation accuracy.

IV. Simulation Results

The packing ratio obtained with our proposed packing ratio estimation algorithms is not arbitrary and could only be $k/U, k = 1, 2, \cdots, U$. Therefore, the probability of false alarm (PFA) is more suitable than the mean squared error (MSE) to assess the accuracy of our proposed packing ratio estimation algorithms. Accordingly, we use the PFA in this section to evaluate the estimation accuracy of the proposed algorithms. We first consider the case with a fixed packing ratio. Then, we investigate the circumstance where each frame adopts a packing ratio randomly. Without loss of generality, the BPSK in 5G is adopted to modulate the pilots. The roll-off factor of the SRRC filter is set to 0.3. The length of a single pilot block and the span of non-coherent correlations are set to 64 and 1, respectively. Moreover, the phase noise is randomly distributed between 0 and 2π, and remains unchanged over each pilot block. Considering that DA-PRE has higher estimation accuracy than NDA-PRE [14], we compare our proposed algorithms with DA-PRE, whose length of symbols used for estimation is set to 5000. Unless otherwise specified, only AWGN channels are applied.

In the absence of frequency offset and phase noise, the estimation performance of the proposed packing ratio estimation algorithms is shown in Fig. 3. It can be observed that the PFA of PRE-CC is lowest for any packing ratio adopted, which implies that PRE-CC has the best estimation performance. Even in low signal-to-noise ratio (SNR) regime, PRE-CC realizes accurate estimation. By contrast, PRE-DPDI and PRE-DGPDI perform worse due to the noise amplification of the PDI operation. Besides, the estimation accuracy of PRE-DGPDI is superior to that of PRE-DPDI. As for DA-PRE, its performance varies greatly with different packing ratios. DA-PRE excels in the low SNR regime; when the packing ratio is 0.6, DA-PRE even outperforms PRE-CC. Besides, the PFA of DA-PRE decreases slower with increasing SNR than our proposed algorithms; therefore, our proposed algorithms have higher estimation accuracy in the high SNR regime. It is worth mentioning that the estimation accuracy of DA-PRE

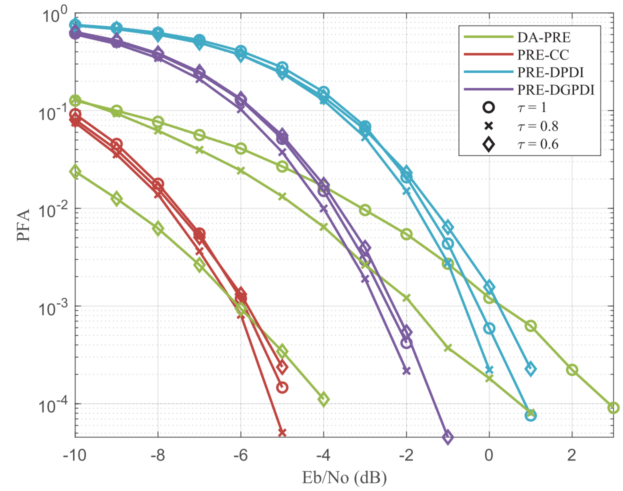

Fig. 3. Estimation performance in the absence of frequency offset and phase noise.

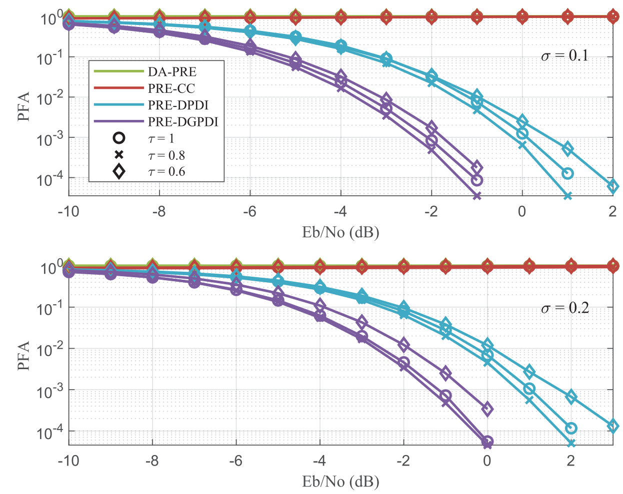

Fig. 4. Estimation performance in the presence of frequency offset and phase noise.

can be improved by increasing K; therefore, DA-PRE is more suitable for FTN signaling with infrequent variations in packing ratios.

In the presence of frequency offset and phase noise, the estimation performance of the proposed packing ratio estimation algorithms is shown in Fig. 4. For the normalized frequency offset of 0.1 and 0.2, the PFA of PRE-CC and DA-PRE no longer decreases as the SNR increases, which means that PRE-CC and DA-PRE are not robust to frequency offset and phase noise. When the normalized frequency offset is 0.1, the estimation performance of PRE-DPDI and PRE-DGPDI is slightly reduced than that in Fig. 3. Comparing the normalized frequency offset of 0.2 with that of 0.1, the estimation performance loss of PRE-DPDI and PRE-DGPDI is about 1 to 2 dB for the PFA of 10^{-4}. Besides, no matter which packing ratio is adopted, PRE-DGPDI achieves the highest robustness and the best estimation accuracy in the presence of frequency offset and phase noise.

From Figs. 3 and 4, the PFA trends of PRE-DPDI and PRE-DGPDI in different FTN-induced ISI cases are consistent for different frequency offsets. Taking PRE-DPDI for instance, the PFA for the packing ratio of 0.6 is the highest, and the PFA for the packing ratio of 0.8 is always the lowest. This instance

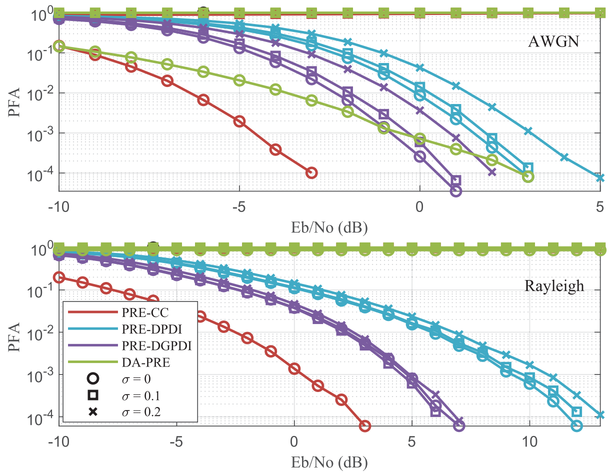

Fig. 5. Estimation performance when the packing ratios are uniformly distributed.

also indicates that the estimation accuracy of PRE-DPDI and PRE-DGPDI is not strongly correlated with the severity of the FTN-induced ISI.

When the packing ratios are uniformly distributed among $[0.6, 0.7, 0.8, 0.9, 1]$, the estimation performance of the proposed packing ratio estimation algorithms over AWGN and Rayleigh channels is shown in Fig. 5. The Rayleigh channel is generated using the RayleighChannel function of Matlab, with a seed of 6 and a maximum Doppler shift of 20 Hz. Note that the upsampling factor for calculating the channel noise equals the upsampling factor of the SRRC filter. From Fig. 5, the estimation performance of the packing ratio estimation algorithms deteriorates as the frequency offset increases. In particular, PRE-CC and DA-PRE are not robust to frequency offset and phase noise, while PRE-DPDI and PRE-DGPDI can effectively mitigate their impacts. Specifically, PRE-DGPDI performs much better than PRE-CC and PRE-DPDI in the presence of frequency offset and phase noise. By comparing the PFA over the Rayleigh channel with that over the AWGN channel, to achieve a PFA of 10^{-4}, the SNR losses of PRE-DPDI and PRE-DGPDI, caused by Rayleigh fading, are about 6 dB and 8 dB. Even so, Fig. 5 indicates that the proposed algorithms can be applied to Rayleigh channels. By contrast, even in the absence of frequency offset and phase noise, the PFA of DA-PRE does not decrease with the increasing SNR in Rayleigh channels.

V. Conclusion

This letter investigated packing ratio estimation for the FTN signaling. Initially, a pilot-based FTN transmission scheme over the channel with frequency offset and phase noise was established. Subsequently, all possible packing ratios were applied for downsampling. By conducting correlation operations on the downsampled pilots, the downsampling factor corresponding to the maximum decision value of the correlation operations was determined. Finally, the packing ratio was obtained. Simulation results demonstrated that, even in the presence of significant frequency offset and phase noise, PRE-DPDI and PRE-DGPDI achieved high estimation accuracy.

References

[1] J. E. Mazo, "Faster-than-Nyquist signaling," *Bell Syst. Tech. J.*, vol. 54, no. 8, pp. 1451–1462, Oct. 1975.

[2] F. Rusek and J. B. Anderson, "Constrained capacities for faster-than-Nyquist signaling," *IEEE Trans. Inf. Theory*, vol. 55, no. 2, pp. 764–775, Feb. 2009.

[3] S. Li, B. Bai, J. Zhou, P. Chen, and Z. Yu, "Reduced-complexity equalization for faster-than-Nyquist signaling: New methods based on ungerboeck observation model," *IEEE Trans. Commun.*, vol. 66, no. 3, pp. 1190–1204, Mar. 2018.

[4] M. Tong, X. Huang, and J. Andrew Zhang, "Faster-than-Nyquist transmission with frame-by-frame decision-directed successive interference cancellation," *IEEE Trans. Commun.*, vol. 71, no. 8, pp. 4851–4861, May 2023.

[5] Y. Ma, N. Wu, J. A. Zhang, B. Li, and L. Hanzo, "Generalized approximate message passing equalization for multi-carrier faster-than-Nyquist signaling," *IEEE Trans. Veh. Technol.*, vol. 71, no. 3, pp. 3309–3314, Mar. 2022.

[6] Z. Liao and F. Liu, "Symbol-level precoding for integrated sensing and communications: A faster-than-Nyquist approach," *IEEE Commun. Lett.*, vol. 27, no. 12, pp. 3210–3214, Dec. 2023.

[7] M.-S. Baek, J. Yun, S. Kwak, H. Lim, Y. Kim, and N. Hur, "Physical layer security based on coded FTN signaling for premium services in satellite digital broadcasting system," in *Proc. IEEE Int. Conf. Consum. Electron. (ICCE)*, Jan. 2017, pp. 147–148.

[8] J. Wang, W. Tang, X. Li, and S. Li, "Filter hopping based faster-than-Nyquist signaling for physical layer security," *IEEE Wireless Commun. Lett.*, vol. 7, no. 6, pp. 894–897, Dec. 2018.

[9] Y. Li, J. Wang, W. Tang, X. Li, and S. Li, "A variable symbol duration based FTN signaling scheme for PLS," in *Proc. 11th Int. Conf. Wireless Commun. Signal Process. (WCSP)*, Xi'an, China, Oct. 2019, pp. 1–5.

[10] S. Sugiura, "Secrecy performance of eigendecomposition-based FTN signaling and NOFDM in quasi-static fading channels," *IEEE Trans. Wireless Commun.*, vol. 20, no. 9, pp. 5872–5882, Sep. 2021.

[11] P. Song, F. Gong, and Q. Li, "Blind symbol packing ratio estimation for faster-than-Nyquist signalling based on deep learning," *Electron. Lett.*, vol. 55, no. 21, pp. 1155–1157, Oct. 2019.

[12] P. Song, N. Zhang, L. Cai, G. Li, T. Wu, and F.-K. Gong, "For security and higher spectrum efficiency: A variable packing ratio transmission system based on faster-than-Nyquist and deep learning," *IEEE Trans. Wireless Commun.*, vol. 22, no. 9, pp. 5898–5913, Jan. 2023.

[13] A. Napolitano, "Cyclostationarity: New trends and applications," *Signal Process.*, vol. 120, pp. 385–408, Mar. 2016.

[14] Z. Bahri, "Robust estimators for faster-than-Nyquist signaling," *IEEE Access*, vol. 10, pp. 13787–13799, 2022.

[15] Q. Li, L. Li, Y. Li, W. Han, X. Li, and D. B. da Costa, "Low-complexity SVD precoding for faster-than-Nyquist signaling using high-order modulations," *IEEE Trans. Aerosp. Electron. Syst.*, vol. 60, no. 1, pp. 591–603, Feb. 2024.